Journal of Membrane Science & Research

journal homepage: www.msrjournal.com

Research Paper

Role of Membrane Technology in Biorefineries - Dehydration of Deep Eutectic Solvent by Pervaporation

Hanna Valkama [1], Esa Muurinen [1], Satu Ojala [1], Juha P. Heiskanen [2], Rafal Sliz [3], Ossi Laitinen [4], Riitta L. Keiski [1,*]

[1] *Research Unit of Environmental and Chemical Engineering, University of Oulu, Finland*
[2] *Research Unit of Sustainable Chemistry, University of Oulu, Finland*
[3] *Optoelectronics and Measurement Techniques Laboratory, University of Oulu, Finland*
[4] *Research Unit of Fiber and Particle Engineering, University of Oulu, Finland*

Article info

Received 2021-12-30
Revised 2022-02-10
Accepted 2022-03-06
Available online 2022-03-06

Keywords

Pervaporation
Deep eutectic solvent
ChCl-urea
Biorefinery
Raman spectroscopy

Highlights

- Pervaporation is a promising method for dehydration of ChCl-urea
- Highest fluxes and removal of water and degradation products shown by PDMS membrane
- Decomposition of ChCl-urea observed at the experimental temperatures of 50–60 °C
- Raman spectroscopy is an excellent tool in the analysis of the ChCl-urea samples

Graphical abstract

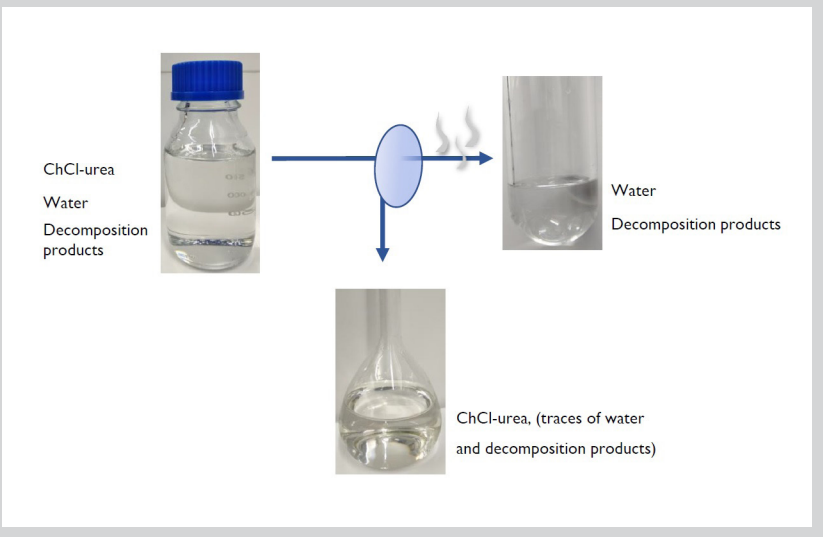

Abstract

In this paper, the dehydration and purification of a deep eutectic solvent choline chloride-urea (ChCl-urea) by pervaporation is presented. The stability of polymeric pervaporation membranes was first studied by exposing the membranes to ChCl-urea for 5 days at 40 °C and 60 °C. The results showed that the membranes were stable when in contact with ChCl-urea and no membrane material was dissolved. In the dehydration experiments, the permeate fluxes were highest with the polydimethylsiloxane (PDMS) membrane: 267.65 g m^{-2} h^{-1} at 50 °C and 413.39 g m^{-2} h^{-1} at 60 °C. Raman spectroscopy was employed in the analysis of the samples. The results also showed the decomposition of ChCl-urea, and the presence of the decomposition products, i.e., ammonia and carbamate, in the PDMS and PDMS-PVA-TiO_2 permeates. With the highest permeate fluxes and simultaneous removal of water and decomposition products, PDMS appeared to be the most promising membrane for the purification and dehydration of ChCl-urea.

© 2022 FIMTEC & MPRL. All rights reserved.

1. Introduction

In this research, dehydration of a class of solvents called deep eutectic solvents (DESs) is investigated. They are relatively new and green media that can be used in biomass processing, for instance. DESs are easy to synthesize, based on readily available bulk chemicals, and biodegradable. [1] The DES system consists of two or more substances that form a eutectic mixture, which has a significantly lower melting point than that of any of its individual components, mainly due to the generation of intermolecular hydrogen bonds [2,3]. One of the most widespread chemicals used for the formation of a DES is choline chloride [2,4]. Choline chloride is an inexpensive, biodegradable, and non-toxic quaternary ammonium salt, which acts as a hydrogen bond acceptor [1,2,4]. Moreover, choline chloride can form a well-known DES in combination with hydrogen bond donors, such as urea.

The economic and environmental importance of the recyclability of ionic liquids (ILs) and DESs has already been addressed in several publications [5–13]. However, the reuse of the ILs and DESs requires the removal of impurities and excess water. Conventional methods for achieving separation

* Corresponding author: riitta.keiski@oulu.fi (R. L. Keiski)

DOI: 10.22079/JMSR.2022.545874.1525

between water and ILs or DESs have included (vacuum) evaporation [8,9,14–16], salting out [17–19], low-pressure CO_2-induced separation [20], crystallization [21], or lyophilization [22]. Dehydration of ionic liquids by pervaporation has been performed in several studies, e.g., dehydration of 1-allyl-3-methylimidazolium chloride [AMIM]Cl [5], 1-butyl-3-methylimidazolium boric tetrafluoride [BMIM]BF_4 during an enzymatic esterification process [23–25], 1-butyl-3-methylimidazolium phosphor hexafluoride [BMIM]PF_6 [25,26], 1-methyl-3-nonylimidazolium phosphor hexafluoride [NMIM]PF_6 [25], 1-hexyl-3-methylimidazolium boric tetrafluoride [HMIM]BF_4 [25], and 1-ethyl-3-methylimidazolium acetate [EMIM]OAc [27]. However, relatively low permeate fluxes have often been reported [5,26,27].

In contrast, the dehydration of deep eutectic solvents by membrane technologies has only been reported in a few papers. For example. Haerens et al. [10] studied the recovery of ethaline (choline chloride-ethylene glycol) by nanofiltration, reverse osmosis, and pervaporation. They found that, in the pressure-driven membrane processes, the osmotic pressure of the concentrated DES limited the removal of water, whereas pervaporation with a PERVAP 2201 membrane showed a low flux and also allowed the permeation of ethylene glycol [10]. To the best knowledge of the authors, the dehydration of ChCl-urea by pervaporation has not been reported before.

This research aimed to find membranes that tolerate ChCl-urea and dehydrate ChCl-urea from residual water to improve its recyclability in the pre-treatment of lignocellulosic materials. This paper reports on the dehydration of ChCl-urea with three different thin-film composite pervaporation membranes and analysis of the samples by Raman spectroscopy. In addition, the resistance of the membranes towards ChCl-urea was tested and evaluated using ^{1}H Nuclear Magnetic Resonance (NMR) measurements, contact angle measurements, Field Emission Scanning Electron Microscopy (FESEM), and Focused Ion Beam–Scanning Electron Microscopy (FIB-SEM).

2. Material and methods

2.1. Materials

In this research, thin-film composite pervaporation membranes were studied. PERVAP 4155-80 membranes were purchased from DeltaMem AG. Polydimethylsiloxane (PDMS) and titanium dioxide (TiO_2) reinforced polyvinyl alcohol (PVA) membranes with a PDMS protective layer was provided by Helmholtz-Zentrum Hereon, Hereon (Geesthacht, Germany). The characteristics of the membranes are presented in Table 1.

Urea (97%) and choline chloride (>98%) for the DES were purchased from Borealis (Austria) and Algry Qu Mica (Spain), respectively. The ChCl-urea DES was produced by oven heating 1620 g of choline chloride and 1223 g of urea in a 5-L beaker at 100 ˚C until the mixture melted. [28] Then, the mixture was placed into a water bath (100 ˚C) under constant stirring for 30 minutes to obtain a clear, colorless liquid. DMSO-d_6 (99.80% D + 0.03% TMS) was purchased from Eurisotop and used as a solvent for the ^{1}H NMR samples.

2.2. ^{1}H NMR analysis

The aim of the ^{1}H NMR analysis was to detect the possible presence of dissolved membrane layer materials in the ChCl-urea after the exposure. To obtain reference NMR spectra for the pure membranes, fresh membrane pieces (30 mg) were immersed into (~800 µL) DMSO-d_6 to dissolve any soluble organic materials. Similarly, a fresh ChCl-urea sample was dissolved into DMSO-d_6 to obtain a reference NMR spectrum for the ChCl-urea. The protocol of the exposure studies was modified from the method presented in García et al. 2013 [5]. Two pieces were cut from each membrane and were submerged in ChCl-urea; one for five days at 40 °C and the other at 60 °C, and the collected ChCl-urea samples were dissolved in DMSO-d_6. The prepared samples were placed in 5 mm NMR tubes and the ^{1}H NMR spectra were recorded using a Bruker Ascend 400 MHz spectrometer and standard proton parameters at ambient temperature.

2.3. Raman spectroscopy

The feed and permeate samples were analyzed using a Timegated® Pico Raman spectrometer. Pico Raman uses a pulsed 532 nm laser source and a CMOS-SPAD detector and is able to measure Raman spectra at 100 ps timescales, minimizing the possible fluorescence background. The Raman spectra were measured in a Raman shift range of 100-2300 cm^{-1}. For quantitative analysis of ChCl and urea, the areas of the peaks at 714.97 cm^{-1} and 1002.51 cm^{-1} were used, representing the symmetric stretching vibration of the four C–N bonds of the *gauche* conformation of choline (ν_{s1}*CN gauche*) and symmetric CN stretching vibrations (ν_{sym} *CN*) of urea, respectively. The peak areas were determined using the Gauss peak function of Origin 2020b software. For the calibration, 18 ChCl-urea samples with concentrations of 0.05, 0.1, 0.25, 0.5, 1.0, 1.25, 2.5, 5.0, 10, 20, 30, 40, 50, 60, 70, 80, 90, and 100 wt.% were prepared and analyzed five times. The calibration line was determined using the known ChCl-urea concentrations and an average of the determined peak areas of five repeated analyses. The standard deviation of the analysis varied from 0.0025 for the low concentrations to 3.15 for the high concentrations. The limit of quantification (LOQ) and the limit of detection (LOD) of the analysis method were defined as 0.1 wt.% and 0.05 wt.%, respectively.

ChCl-urea is known to be hygroscopic; however, in the pre-treatment of lignocellulosic materials and in the pervaporation experiments it is impossible to avoid contact with ambient air, and thus it will always contain some water. Therefore, the calibration samples were prepared only by using fresh DES without further drying but with minimal exposure to ambient air. Hence, these results are closer to the real process where the DES is used in the pre-treatment of lignocellulosic materials, but they still allow the determination of the relative changes in the compositions of the feed and permeate streams.

2.4. Contact angle measurements

Contact angle measurements were made for both fresh and exposed membranes to detect the possible differences in the hydrophilicity before and after contact with ChCl-urea. The interactions between water and membranes were analyzed by using a static contact angle measurement system – the Kruss DSA100 (Germany). The system was equipped with a high-speed camera (64 fps) and designated Kruss analyzing software. The experiments were conducted at room temperature, using deionized water. To extract the value of the contact angle, a height-width method was used, where the shape of the sessile drop describes a circular arc on the surface. The value of the contact angle was calculated from the height and width of the rectangle which encloses the circular arc. For each membrane, three separate measurements were conducted at different locations, the results were averaged, and the standard deviation was calculated.

2.5. Field emission scanning electron microscope imaging

Field emission scanning electron microscopy (FESEM) was performed to observe whether the ChCl-urea exposure had changed the membrane surface or detached the active layer. FESEM images of fresh and exposed membranes were taken with a Zeiss Ultra Plus device. Prior to imaging, the membrane surface was coated by platinum sputtering for 30 s at 40 mA.

2.6. Focused ion beam–scanning electron microscope measurements

Focused ion beam–scanning electron microscope (FIB-SEM) measurements were performed on the fresh and exposed membranes to observe any possible changes in the thickness of the membrane active layer. Prior to the measurements, the membrane surface was coated by platinum sputtering for 60 s at 40 mA. The FIB-SEM measurements were performed with dual-beam FEI Helios NanoLab 600 equipment. The thicknesses of the membrane active layers were measured from several different locations, the results were averaged, and the standard deviation was calculated.

Table 1
Studied pervaporation membranes and their characteristics as given by the manufacturers.

Membrane	Manufacturer	Active layer	Support material
PERVAP 4155-80	DeltaMem AG	Cross-linked copolymers with PVA	
PDMS	Hereon	PDMS	PAN on PES non-woven
PDMS-PVA-TiO_2	Hereon	TiO_2 reinforced PVA with PDMS protection layer	PPSU on PPS non-woven

2.7 Pervaporation experiments

The dehydration experiments were performed with a laboratory-scale P28 cross-flow membrane unit (CM-CELFA Membrantrenntechnik AG, Switzerland) (Fig. 1). The effective membrane area is 2.8×10^{-3} m^2 and the maximum feed volume is 500 mL. The equipment operates in batch mode,

i.e., the retentate is circulated to the feed tank while the permeate is removed from the system. The temperature of the feed solution was maintained at 50, 55, or 60 °C using a Lauda Ecoline Staredition E 103 thermostatic unit. The feed stream was circulated with a Scherzinger 3000 3B/M gear pump equipped with a frequency converter. The ChCl-urea feed flow rates at the experimental temperatures of 50, 55, and 60 °C were 0.25, 0.28, and 0.31 L/min, respectively. The permeate side pressure was maintained at 1 mbar with a rotary-vane Varian DS 302 vacuum pump. The permeate was removed and condensed in liquid nitrogen cryo traps. The feed stream contained 90 wt.% ChCl-urea and 10 wt.% water. To achieve the desired conditions, the system was conditioned for 1 hour prior to each experiment. Each experiment lasted for 4 hours. Samples were taken from the initial feed solution, regularly from the feed and permeate during the experiment, and eventually from the remaining feed solution. The pH was measured from the initial and the remaining feed samples with a VWR pHenomenal pH 1000 L pH meter.

The experimental plan was created using MODDE 12.1 Pro software (Sartorius Stedim Data Analytics AB). The variables of the screening model were membrane and temperature (T) and the responses were the total permeate flux (J_T) and permeate water concentration (c_{wp}).

2.8 Calculations of membrane performance

The mass transfer in pervaporation is described by the solution-diffusion model, and the driving force can be expressed as a gradient in the vapor pressure between the liquid feed and the permeate vapor. The flux of compound i through the membrane can be defined as $J_i = Q_i\,(p_{i,f} - p_{i,p})$, where Q_i is the membrane permeance. The partial vapor pressures $p_{i,f}$ and $p_{i,p}$ of the compound i in the feed and permeate side can be defined by the extended Raoult's law: $p_{i,f} = \gamma_i\, x_{i,f}\, p_i^0$, where γ_i is the activity coefficient of the compound i, $x_{i,f}$ is the mole fraction of the compound i in the feed, and p_i^0 is the vapor pressure of the pure compound i. The vapor pressure of compound i on the permeate side can be defined as $p_{ip} = y_{ip}\, p^p$, where $y_{i,p}$ is the mole fraction of the compound i in the permeate, and p^p is the permeate side pressure.

The experimental permeate flux was calculated using the equation $J = m/(tA)$, where m is the mass of a permeate sample during time t and A is the effective membrane area. The separation factor of water and ChCl-urea was calculated as follows:

$$\beta_i = \frac{C_{ip}/(1-C_{ip})}{C_{if}/(1-C_{if})} \tag{1}$$

where c_{ip} is the concentration of the compound i in the permeate and c_{if} is the concentration of the compound i in the feed. The vapor pressure of ChCl-urea on the feed side was calculated using the Antoine equation:

$$\ln p_{i,f} = h_1 - \frac{h_2}{T + h_3} \tag{2}$$

where $p_{i,,f}$ is the vapor pressure (mmHg), T is the temperature (K), and h_i's are parameters presented by Wu et al. [29].

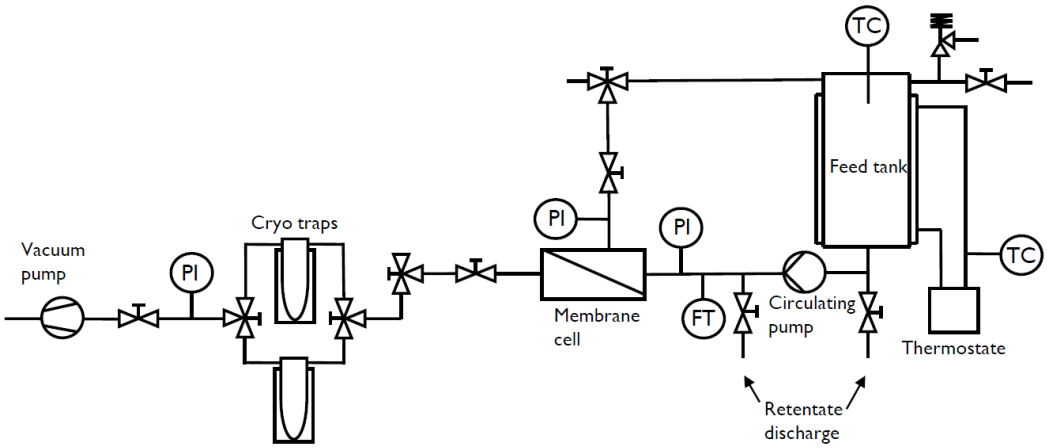

Fig. 1. Experimental setup of the pervaporation unit.

3. Results and discussion

3.1 Effect of ChCl-urea on membrane properties

3.1.1 NMR analysis

The ^{1}H NMR spectra of the fresh ChCl-urea and the ChCl-urea samples after the exposure tests along with PERVAP 4155-80 in DMSO-d_6 are presented in Fig. 2. The assignment of the ChCl-urea spectrum (i in Fig. 2) in DMSO-d_6 was based on the previous assignment presented by Delso et al. [30]. The trace water signal was assigned to around 3.36 ppm, based on the NMR chemical shifts of trace impurities reported by Fulmer et al. [31]. The ^{1}H NMR spectrum of PERVAP 4155-80 (iv in Fig. 2) shows weak signals of the PVA polymer. The peak of CH_2 protons of PVA appears at around 1.38 ppm, CH at 3.83 ppm, and the trace peaks of OH proton appear at 4.22, 4.46, and 4.65 ppm [32]. The unidentified component of PERVAP 4155-80 shows the main peaks at 2.03 and 3.14 ppm. The exposed ChCl-urea samples (ii and iii in Fig. 2) show only signals corresponding to ChCl-urea. Similar analyses were carried out for the PDMS and PDMS-PVA-TiO_2 membranes; the comparisons of ^{1}H NMR spectra are presented in Figs. A.1 and A.2. Based on the ^{1}H NMR analyses, all three membranes seem to be stable under the studied exposure conditions.

3.1.2 Field emission scanning electron microscope imaging

The FESEM images of the fresh and exposed membranes are presented in Fig. 3. No changes were observed in the PERVAP 4155-80 membrane surface after exposure. However, the surface of the PDMS-PVA-TiO_2 membrane became wrinkled after exposure at 60 °C. At some locations, the surface of the PDMS membrane after the exposure looked slightly more porous than the fresh membrane, especially when several images were taken sequentially at the 5,000x–10,000x magnifications. One reason for these changes might be swelling caused by the dissolved ChCl-urea inside the membrane structure. On the other hand, the PDMS membrane was very sensitive towards the electron beam in SEM. In addition, some samples (Fig. A.3) appeared to contain a higher amount of residual ChCl-urea in the membrane. However, it cannot be concluded from these FESEM images whether the ChCl-urea exists on the top or bottom surface or inside the membrane structure, and if the latter, in which membrane layer in particular it exists. Additionally, in the exposure studies, the whole membrane samples were immersed in ChCl-urea, whereas during the pervaporation experiments, only the membrane active layer was in contact with the ChCl-urea feed stream.

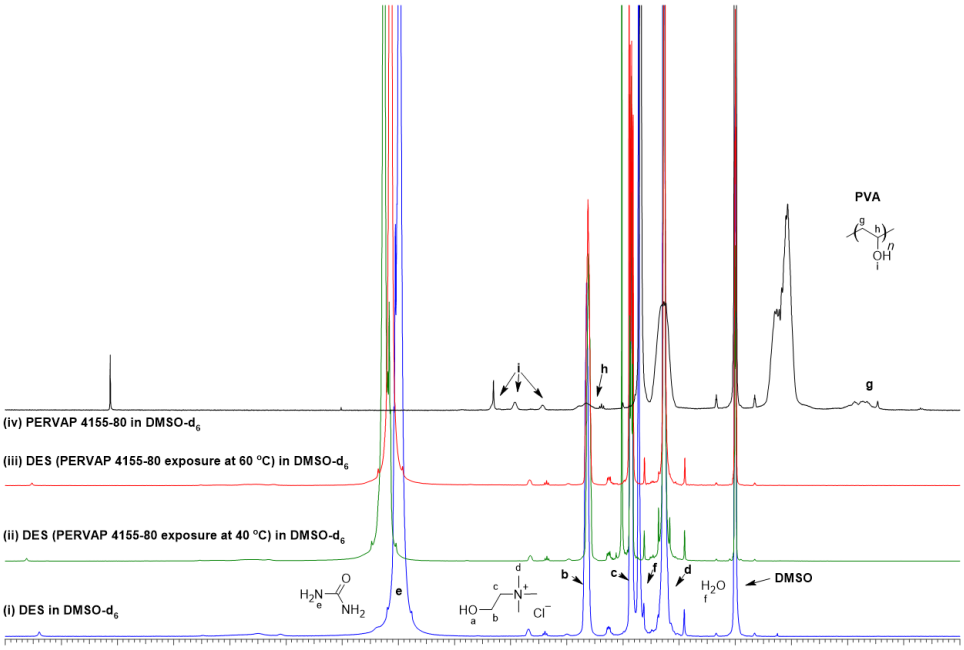

Fig. 2. ^{1}H NMR spectra of fresh DES (i), exposed DES samples (ii and iii), and PERVAP 4155-80 (iv) in DMSO-d_6.

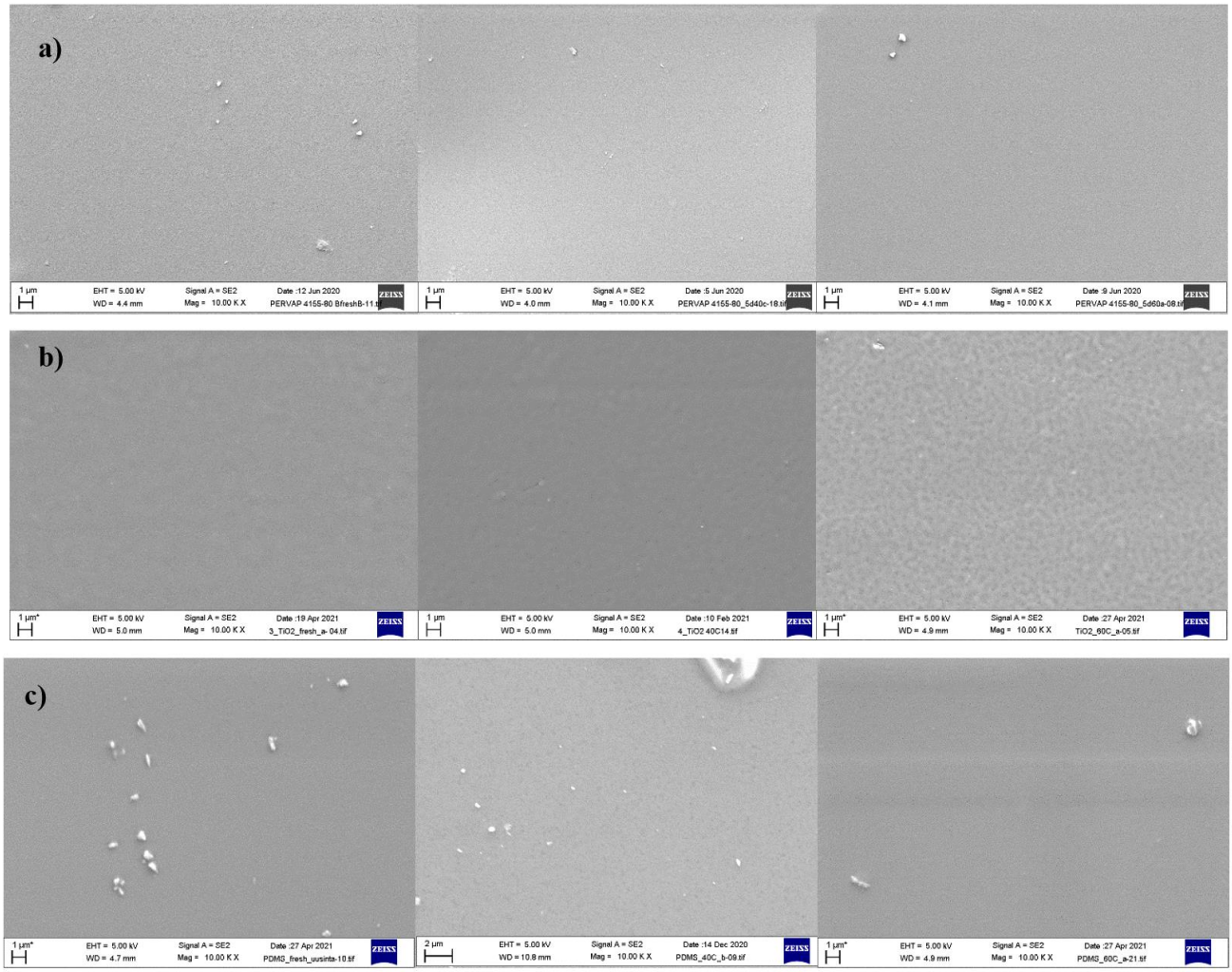

Fig. 3. FESEM images at 10,000 x magnification of a) PERVAP 4155-80, b) PDMS-PVA-TiO_2, and c) PDMS membranes before (left), after exposure to ChCl-urea at 40 °C (middle), and after exposure at 60 °C (right).

3.1.3. Focused ion beam–scanning electron microscope measurements

The results from the FIB-SEM measurements are presented in Table 2 and Figs. A.4–A.6.

The results show that the thicknesses of the membrane active layers did not decrease during the exposure to ChCl-urea, confirming the ^{1}H NMR results that no membrane material was dissolved. On the contrary, the thicknesses of the active layer of each membrane increased, indicating swelling, i.e., an increase in the volume of the membrane caused by the dissolution of solutes into the membrane polymer. Severe swelling, while increasing permeability, may decrease the selectivity of the membrane or, at worst, even change the nature of the mass transfer from diffusive towards convective [33]. The presence of ChCl-urea inside the membrane active layer can be best observed in Fig. A.6.b-d, after the contact of the PDMS-PVA-TiO_2 membrane with ChCl-urea. These FIB-SEM images complement the FESEM images, verifying the existence of ChCl-urea, particularly inside the active layer. As a comparison, the thicknesses of the membranes used in the pervaporation experiments were measured. The average thicknesses of the PDMS-PVA-TiO_2 and PDMS active layers after the pervaporation experiments were between the thicknesses after the exposures at 40 °C and 60 °C. In contrast, the active layer of the PERVAP 4155-80 was thicker than in the exposure tests, and 83% thicker than that of the fresh membrane, hence indicating an even higher degree of swelling during the pervaporation experiments. This may be due to the 10% water concentration in the basic ChCl-urea feed stream which may have increased the degree of swelling of the hydrophilic PERVAP 4155-80 membrane, whereas it did not have an effect on the hydrophobic PDMS-PVA-TiO_2 and PDMS membranes. This suggestion is supported by observations by Angelini et al. [34]. According to their observations, an increase in the water concentration of a basic feed stream increased the swelling of the hydrophilic PERVAP 4155-30 and PERVAP 4155-70 membranes, which are similar to the PERVAP 4155-80 membrane used in this study, apart from different ratios of PVA and the copolymers [34]. In their swelling studies with ionic liquids, Izak et al. [35] also observed that the degree of swelling of a Nafion membrane was higher in a binary mixture of IL and H_2O than with each component separately. The FIB-SEM results also show the combined effect of both ChCl-urea and water on the swelling of hydrophilic membranes.

3.1.4 Contact angle measurements

The contact angle results are presented in Table 3. The relatively low values of standard deviation indicate the stable behavior of the samples and homogeneity of the treatments.

Table 3 shows a decrease in the water contact angles of the PV membranes: 78% for PERVAP 4155-80 and around 6% for PDMS and PDMS-PVA-TiO_2, caused by the exposure to ChCl-urea, indicating an increase in hydrophilicity or a decrease in hydrophobicity, respectively. The increase in hydrophilicity may predict higher selectivity towards the water. Table 3 also shows that higher temperatures produced a higher increase in hydrophilicity. The water contact angles of the fresh membranes are in good correlation with other reported values of 45.3° [36] and 105.5–128° [37–40] for the PERVAP 4155 (different amounts of PVA and copolymer) and PDMS materials, respectively. Since the PDMS-PVA-TiO_2 has a PDMS protection layer on its surface, its contact angle was compared to the PDMS and not to the PVA and TiO_2 materials.

3.2. Dehydration of ChCl-urea

The permeate fluxes were lowest with the PERVAP 4155-80 membrane and highest with the PDMS membrane (Table 4). As expected, the increase in the experimental temperature increased the fluxes. All these fluxes are higher than the reported fluxes of ~30 g $m^{-2}h^{-1}$ in the dehydration of Ethaline [10] and 3.39 g $m^{-2}h^{-1}$ in the dehydration of [AMIM]Cl at 60 °C [5] from a feedwater concentration of 10 %; however, the experimental temperatures were not reported in [10]. Schäfer et al. obtained a flux of ~ 18 g $m^{-2}h^{-1}$ in the dehydration of [BMIM]PF_6 with a feed water concentration of 17 g/L at 50 °C [26]. Sun et al. [27], reported permeate fluxes of 400–500 g $m^{-2}h^{-1}$ in dehydration of 20% [EMIM]OAc at 50 °C. Nevertheless, any comparisons are only indicative due to differences in the experimental setups, membranes, feed compositions, and operating conditions.

The measured Raman spectrum of ChCl-urea is presented in Fig. A.7. The highest Raman band at 1002.51 cm^{-1} is assigned to the symmetric CN stretching vibrations (ν_{sym} *CN*) of urea. The second highest peak at 714.97 cm^{-1} is assigned to the symmetric stretching vibration of the four C–N bonds of the *gauche* conformation of choline (ν_{s1}*CN gauche*). [41–44] These two bands were monitored in the quantification. Other characteristic peaks were also monitored, and they are assigned in Table A.1. The calibration line is presented in Fig. A.8.

The characteristic bands of choline and urea were not detected in any of the permeate samples, and the PERVAP 4155-80 permeate Raman spectra were identical to those of pure water samples. Therefore, it can be concluded that swelling did not have a detrimental effect on the selectivity of the membrane. However, extra peaks (Fig. 4) were detected in the permeate samples in the experiments with PDMS and PDMS-PVA-TiO_2, most likely due to the decomposition of ChCl-urea into carbachol (bands 1036 and 1070 cm^{-1}: NH_2 wag of H_2NCOO^-, (ω NH_2) [45], and symmetric CO stretching vibration (ν_{sym} *CO*) [46], respectively) and ammonia (band 1117 cm^{-1}). Also, the CN stretching vibration of H_2NCOO^- (ν *CN*) can appear at 1120 cm^{-1} [45]. Due to the absence of the choline and urea bands, Fig. 4 shows permeation of only water, ammonia, and carbamate, which can further react to carbonate in presence of ammonia [47]. The presence of ammonia was verified by recording the Raman spectra of 1, 5, 10, and 25% ammonia solutions and comparing the resulting spectra with the permeate spectra; however, the concentrations were not quantified. These observations indicate the decomposition of ChCl-urea already at the experimental temperature range of 50–60 °C, but they may also originate from the preparation of ChCl-urea DES at 100 °C. In the presence of impurities/other compounds, ChCl-urea has been reported to partially decompose at 80 °C [48,49]; however, no systematic studies of the decomposition of ChCl-urea were found. The decomposition products could not be detected in any of the feed samples, or at least their concentrations may have been so small that they were overpowered by the strong ChCl and urea bands.

Vapor pressures of water, ChCl-urea, ammonia, and carbachol are collected in Table 5. Since the data for the vapor pressure calculations of the mixture (p_{if}'s) was found only for 80 wt.% ChCl-urea solutions from [29], the numbers are only indicative. The vapor pressures of water and ammonia are significantly higher than that of ChCl-urea, and hence their permeation is more favorable. This verifies the observations about the presence of water and ammonia in the permeate Raman spectra.

Table 2
Thicknesses (μm) of the membrane active layers before and after exposure to ChCl-urea and after the pervaporation experiments.

	PERVAP 4155-80				PDMS				PDMS-PVA-TiO_2			
	Fresh	40 °C	60 °C	PV experiment	Fresh	40 °C	60 °C	PV experiment	Fresh	40 °C	60 °C	PV experiment
Average	1.30	2.12	1.89	2.38	1.92	2.49	2.08	2.05	2.66	2.66	3.06	2.79
St. Dev.	0.10	0.09	0.04	0.13	0.32	0.36	0.09	0.18	0.64	0.19	0.23	0.10

Table 3
Contact angles (°) of the pervaporation membranes before and after exposure to ChCl-urea at 40 °C and 60 °C.

	PERVAP 4155-80 fresh	PERVAP 4155-80 40 °C	PERVAP 4155-80 60 °C	PDMS fresh	PDMS 40 °C	PDMS 60 °C	PDMS-PVA-TiO_2 fresh	PDMS-PVA-TiO_2 40 °C	PDMS-PVA-TiO_2 60 °C
Average	43.87	13.83	9.57	112.77	107.83	105.90	109.33	103.15	102.90
St. Dev.	0.31	1.40	1.76	0.12	0.92	0.72	0.40	1.72	0.88

Table 4
Pervaporation experiments include experimental permeate fluxes and ChCl-urea concentrations.

Membrane	T (°C)	Permeate flux (g $m^{-2}h^{-1}$)	St. Error	Permeate ChCl-urea concentration (%)
PERVAP 4155-80	50	58.04	± 2.14	≤ 0.05
PERVAP 4155-80	55	71.43	± 2.14	≤ 0.05
PERVAP 4155-80	55	65.18	± 2.14	≤ 0.05
PERVAP 4155-80	60	107.14	± 2.14	≤ 0.05
PDMS-PVA-TiO_2	50	178.57	± 2.14	≤ 0.05
PDMS-PVA-TiO_2	60	214.08	± 2.14	≤ 0.05
PDMS	50	267.64	± 2.14	≤ 0.05
PDMS	60	413.39	± 2.14	≤ 0.05

Table 5
Vapor pressures of water, ChCl-urea, and ammonia. p_{if}'s were calculated for a mixture containing 80 wt.% ChCl-urea.

Compound	p_i^0 (mbar)	$p_{i,f}$ (mbar)
Water	123.44 [50]	90.64*
ChCl-urea	-	2.76 **
Ammonia	287 [51]	-

* Calculated using Raoult's law, value for γ_w from [29].
** Calculated using Antoine equation, (Eq. 2), values for h_i's from [29].

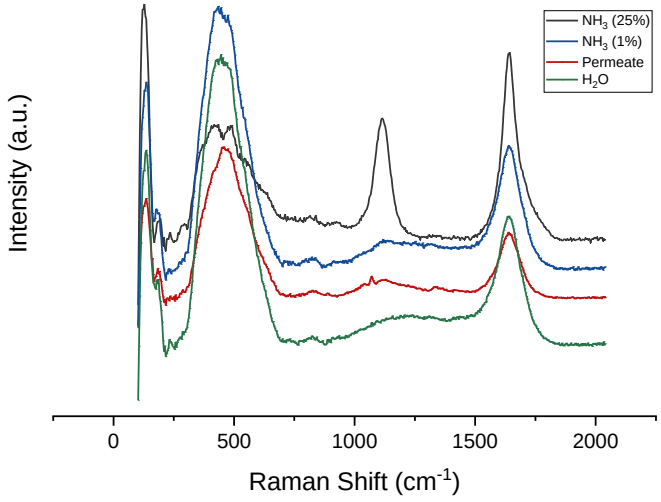

Fig. 4. Comparison of the Raman spectra of PDMS permeate to 25% and 1% NH_3 and pure DI water.

4. Conclusions

This study shows that pervaporation is a promising method for the dehydration of ChCl-urea, and stable membranes in the presence of ChCl-urea were found. According to these results, ChCl-urea did not dissolve the active layers of the studied membranes. However, the swelling was observed in all membranes after being in contact with ChCl-urea and a ChCl-urea-water solution. PERVAP 4155-80 showed high selectivity towards the water, but the permeate fluxes were significantly lower than with the other two membranes. The PDMS membrane showed the highest permeate fluxes; 1.5 x higher than PDMS-PVA-TiO_2 and 4 x higher than PERVAP 4155-80.

Raman spectroscopy was employed in the analysis of ChCl-urea samples and it proved to be a promising method for this kind of application. ChCl-urea was not detected in any of the permeate samples. On the other hand, decomposition products of ChCl-urea were detected in the permeate samples of PDMS and PDMS-PVA-TiO_2, indicating the partial decomposition of ChCl-urea during the preparation or pervaporation process. However, their concentrations were relatively small. Because ChCl-urea may not be fully stable under the experimental temperatures of 50–100 °C, mild temperatures are recommended for actions where ChCl-urea is used.

Since the aim of this study was to enable the re-use of ChCl-urea, the removal of the degradation products along with water is highly beneficial for the overall process. Hence, the PDMS membrane, with the simultaneous removal of water and the degradation products, and with the highest permeate fluxes was the most promising membrane for the dehydration and purification of ChCl-urea. Therefore, it could also be the most feasible membrane from the industrial point of view. Future research should be concentrated particularly on the performance of the membranes during a long-term dehydration process. In addition, to avoid or minimize the decomposition of ChCl-urea and to increase the membrane lifetime, dehydration with the PDMS membrane at lower temperatures merits study.

Acknowledgments

The authors would like to thank the EU and the Council of Northern Ostrobothnia for financing the project under the frame of the European Regional Development Fund (ERDF) (Project number: A73930). The authors would also like to thank the project partners Kai-Cell Fibers Oy, Stora Enso Oulu Oy, Kemira Oyj, Kiertokaari Oy, and Pölkky Oyj for funding the project. Part of the work was carried out with the support of the Center of Microscopy and Nanotechnology, University of Oulu, Finland, and Mr. Esa Heinonen is acknowledged for the FIB-SEM measurements. Dr. Torsten Brinkmann from Helmholtz-Zentrum Hereon, Hereon is acknowledged for kindly providing membranes for this research. The authors are grateful to Dr. Minna Tiainen, Ms. Auli Turkki, and Ms. Anni Lenkola for valuable advice, and Mr. Ismo Koskenkorva, Ms. Noora Nyman, Ms. Annika Kerola, Mr. Jarmo Murto, and Mr. Raimo Tervola for assisting during the laboratory experiments and with the used equipment. Pelc Southbank Languages Ay is acknowledged for English proofreading of the manuscript.

Abbreviations

A	Effective membrane area [m^2]
[AMIM]Cl	1-Allyl-3-methylimidazolium chloride
[BMIM]BF_4	1-Butyl-3-methylimidazolium boric tetrafluoride
[BMIM]PF_6	1-Butyl-3-methylimidazolium phosphor hexafluoride
ChCl-urea	Choline chloride-urea
DES	Deep eutectic solvent
DMSO-d_6	Deuterated dimethyl sulfoxide
[EMIM]OAc	1-Ethyl-3-methylimidazolium acetate
FESEM	Field emission scanning electron microscope
FIB–SEM	Focused ion beam–scanning electron microscope
[HMIM]BF_4	1-Hexyl-3-methylimidazolium boric tetrafluoride
[NMIM]PF_6	1-Methyl-3-nonylimidazolium phosphor hexafluoride
NMR	Nuclear magnetic resonance
PAN	Polyacrylo nitrile
PDMS	Polydimethylsiloxane
PES	Polyester
PPS	Poly phenylene sulphide
PPSU	Poly phenylene sulfone
PVA	Polyvinyl alcohol
TiO_2	Titanium dioxide
TMS	Tetramethyl silane

References

[1] A.P. Abbott, G. Capper, D.L. Davies, R.K. Rasheed, V. Tambyrajah, Novel solvent properties of choline chloride/urea mixtures, Chem. Commun. (2003) 70–71. https://doi.org/10.1039/b210714g.
[2] A.P. Abbott, T.J. Bell, S. Handa, B. Stoddart, O-Acetylation of cellulose and monosaccharides using a zinc-based ionic liquid, Green Chem. 7 (2005) 705–707. https://doi.org/10.1039/b511691k.
[3] M. Sharma, C. Mukesh, D. Mondal, K. Prasad, Dissolution of α-chitin in deep eutectic solvents, RSC Adv. 3 (2013) 18149–18155. https://doi.org/10.1039/c3ra43404d.
[4] Q. Zhang, M. Benoit, K. de Oliveira Vigier, J. Barrault, F. Jérôme, Green and inexpensive choline-derived solvents for cellulose decrystallization, Chem. Eur. J. 18 (2012) 1043–1046. https://doi.org/10.1002/chem.201103271.
[5] V. García, H. Valkama, R. Sliz, A.W.T. King, R. Myllylä, I. Kilpeläinen, R.L. Keiski, Pervaporation recovery of [AMIM]Cl during wood dissolution; effect of [AMIM]Cl properties on the membrane performance, J. Membr. Sci. 444 (2013) 9–15. https://doi.org/10.1016/j.memsci.2013.05.010.
[6] J. Zhou, H. Sui, Z. Jia, Z. Yang, L. He, X. Li, Recovery and purification of ionic liquids from solutions: A review, RSC Adv. 8 (2018) 32832–32864. https://doi.org/10.1039/c8ra06384b.

[7] O. Kuzmina, Methods of IL Recovery and Destruction, in: O. Kuzmina, J.P. Hallett (Eds.), Application, Purification, and Recovery of Ionic Liquids, Elsevier Inc., (2016) 205–248. https://doi.org/10.1016/B978-0-444-63713-0.00005-5.

[8] A.P. Parviainen, Acid-base conjugate ionic liquids in lignocellulose processing: synthesis, properties and applications, (2016). http://urn.fi/URN:ISBN:978-951-51-2519-4.

[9] A. Parviainen, R. Wahlström, U. Liimatainen, T. Liitiä, S. Rovio, J.K.J. Helminen, U. Hyväkkö, A.W.T. King, A. Suurnäkki, I. Kilpeläinen, Sustainability of cellulose dissolution and regeneration in 1,5-diazabicyclo[4.3.0]non-5-enium acetate: A batch simulation of the IONCELL-F process, RSC Advances. 5 (2015) 69728–69737. https://doi.org/10.1039/c5ra12386k.

[10] K. Haerens, S. van Deuren, E. Matthijs, B. van der Bruggen, Challenges for recycling ionic liquids by using pressure driven membrane processes, Green Chem. 12 (2010) 2182–2188. https://doi.org/10.1039/c0gc00406e.

[11] B. Wu, W.W. Liu, Y.M. Zhang, H.P. Wang, Do we understand the recyclability of ionic liquids?, Chem. Eur. J. 15 (2009) 1804–1810. https://doi.org/10.1002/chem.200801509.

[12] A. Isci, M. Kaltschmitt, Recovery and recycling of deep eutectic solvents in biomass conversions: a review, Biomass Convers. Biorefin. (2021). https://doi.org/10.1007/s13399-021-01860-9.

[13] R. Wahlström, K. Rommi, P. Willberg-Keyriläinen, D. Ercili-Cura, U. Holopainen-Mantila, J. Hiltunen, O. Mäkinen, H. Nygren, A. Mikkelson, L. Kuutti, High yield protein extraction from brewer's spent grain with novel carboxylate salt - urea aqueous deep eutectic solvents, ChemistrySelect. 2 (2017) 9355–9363. https://doi.org/10.1002/slct.201701492.

[14] X. Wang, H. Li, Y. Cao, Q. Tang, Cellulose extraction from wood chip in an ionic liquid 1-allyl-3-methylimidazolium chloride (AmimCl), Bioresour. Technol. 102 (2011) 7959–7965. https://doi.org/10.1016/j.biortech.2011.05.064.

[15] K.H. Kim, T. Dutta, J. Sun, B. Simmons, S. Singh, Biomass pretreatment using deep eutectic solvents from lignin-derived phenols, Green Chem. 20 (2018) 809–815. https://doi.org/10.1039/c7gc03029k.

[16] J.L.K. Mamilla, U. Novak, M. Grilc, B. Likozar, Natural deep eutectic solvents (DES) for fractionation of waste lignocellulosic biomass and its cascade conversion to value-added bio-based chemicals, Biomass Bioenergy. 120 (2019) 417–425. https://doi.org/10.1016/j.biombioe.2018.12.002.

[17] K.E. Gutowski, G.A. Broker, H.D. Willauer, J.G. Huddleston, R.P. Swatloski, J.D. Holbrey, R.D. Rogers, Controlling the aqueous miscibility of ionic liquids: Aqueous biphasic systems of water-miscible ionic liquids and water-structuring salts for recycle, metathesis, and separations, J. Am. Chem. Soc. 125 (2003) 6632–6633. https://doi.org/10.1021/ja0351802.

[18] C. Li, J. Han, Y. Wang, Y. Yan, J. Pan, X. Xu, Z. Zhang, Phase behavior for the aqueous two-phase systems containing the ionic liquid 1-butyl-3-methylimidazolium tetrafluoroborate and kosmotropic salts, J. Chem. Eng. Data. 55 (2010) 1087–1092. https://doi.org/10.1021/je900533h.

[19] A.F.M. Cláudio, C.F.C. Marques, I. Boal-Palheiros, M.G. Freire, J.A.P. Coutinho, Development of back-extraction and recyclability routes for ionic-liquid-based aqueous two-phase systems, Green Chem. 16 (2014) 259–268. https://doi.org/10.1039/c3gc41999a.

[20] A.M. Scurto, S.N.V.K. Aki, J.F. Brennecke, Carbon dioxide induced separation of ionic liquids and water, Chem. Commun. 3 (2003) 572–573. https://doi.org/10.1039/b211376g.

[21] Q. Yu, Z. Song, X. Zhuang, L. Liu, W. Qiu, J. Shi, W. Wang, Y. Li, Z. Wang, Z. Yuan, Catalytic conversion of herbal residue carbohydrates to furanic derivatives in a deep eutectic solvent accompanied by dissolution and recrystallisation of choline chloride, Cellulose. 26 (2019) 8263–8277. https://doi.org/10.1007/s10570-019-02372-6.

[22] K.M. Jeong, M.S. Lee, M.W. Nam, J. Zhao, Y. Jin, D.K. Lee, S.W. Kwon, J.H. Jeong, J. Lee, Tailoring and recycling of deep eutectic solvents as sustainable and efficient extraction media, J. Chromatogr. A. 1424 (2015) 10–17. https://doi.org/10.1016/j.chroma.2015.10.083.

[23] L. Gubicza, N. Nemestóthy, T. Fráter, K. Bélafi-Bakó, Enzymatic esterification in ionic liquids integrated with pervaporation for water removal, Green Chem. 5 (2003) 236–239. https://doi.org/10.1039/b211342m.

[24] P. Izák, N.M.M. Mateus, C.A.M. Afonso, J.G. Crespo, Enhanced esterification conversion in a room temperature ionic liquid by integrated water removal with pervaporation, Sep. Purif. Technol. 41 (2005) 141–145. https://doi.org/10.1016/j.seppur.2004.05.004.

[25] K. Bélafi-Bakó, N. Dörmő, O. Ulbert, L. Gubicza, Application of pervaporation for removal of water produced during enzymatic esterification in ionic liquids, Desalination. 149 (2002) 267–268. https://doi.org/10.1016/S0011-9164(02)00781-6.

[26] T. Schäfer, C.M. Rodrigues, C.A.M. Afonso, J.G. Crespo, Selective recovery of solutes from ionic liquids by pervaporation—a novel approach for purification and green processing, Chem. Commun. 1 (2001) 1622–1623. https://doi.org/10.1039/b104191f.

[27] J. Sun, J. Shi, N.V.S.N. Murthy Konda, D. Campos, D. Liu, S. Nemser, J. Shamshina, T. Dutta, P. Berton, G. Gurau, R.D. Rogers, B.A. Simmons, S. Singh, Efficient dehydration and recovery of ionic liquid after lignocellulosic processing using pervaporation, Biotechnol. Biofuels. 10 (2017). https://doi.org/10.1186/s13068-017-0842-9.

[28] O. Laitinen, T. Suopajärvi, M. Österberg, H. Liimatainen, Hydrophobic, superabsorbing aerogels from choline chloride-based deep eutectic solvent pretreated and silylated cellulose nanofibrils for selective oil removal, ACS Appl. Mater. Interfaces. 9 (2017) 25029–25037. https://doi.org/10.1021/acsami.7b06304.

[29] S.-H. Wu, A.R. Caparanga, R.B. Leron, M.-H. Li, Vapor pressure of aqueous choline chloride-based deep eutectic solvents (ethaline, glyceline, maline and reline) at 30-70 °C, Thermochim. Acta. 544 (2012) 1–5. https://doi.org/10.1016/j.tca.2012.05.031.

[30] I. Delso, C. Lafuente, J. Muñoz-Embid, M. Artal, NMR study of choline chloride-based deep eutectic solvents, J. Mol. Liq. 290 (2019) 111236. https://doi.org/10.1016/j.molliq.2019.111236.

[31] G.R. Fulmer, A.J.M. Miller, N.H. Sherden, H.E. Gottlieb, A. Nudelman, B.M. Stoltz, J.E. Bercaw, K.I. Goldberg, NMR chemical shifts of trace impurities: Common laboratory solvents, organics, and gases in deuterated solvents relevant to the organometallic chemist, Organometallics. 29 (2010) 2176–2179. https://doi.org/10.1021/om100106e.

[32] S. Hu, F. Hoxu, H. Odani, 1H NMR Study of the solvation and gelation in a poly(vinyl alcohol)/DMSO-d6/H_2O system, Bull. Inst. Chem. Res. Kyoto Univ. 67 (1989) 239–248.

[33] T. Schäfer, J.P.G. Crespo, Vapor Permeation and Pervaporation, in: C.A.M. Afonso, J.P.G Crespo (Eds.), Green Separation Processes: Fundamentals and Applications, Wiley-VCH, Weinheim, (2005) 271–289. https://doi.org/10.1002/3527606602.

[34] A. Angelini, C. Fodor, W. Yave, L. Leva, A. Car, W. Meier, pH-Triggered Membrane in Pervaporation Process, ACS Omega. 3 (2018) 18950–18957. https://doi.org/10.1021/acsomega.8b03155.

[35] P. Izák, Š. Hovorka, T. Bartovský, L. Bartovská, J.G. Crespo, Swelling of polymeric membranes in room temperature ionic liquids, J. Membr. Sci. 296 (2007) 131–138. https://doi.org/10.1016/j.memsci.2007.03.022.

[36] A. Esmaeili, D.W. Kirk, Water removal in the alkaline electrochemical valorization of glycerol by pervaporation, Sep. Purif. Technol. 248 (2020). https://doi.org/10.1016/j.seppur.2020.116943.

[37] R.N. Palchesko, L. Zhang, Y. Sun, A.W. Feinberg, Development of Polydimethylsiloxane Substrates with Tunable Elastic Modulus to Study Cell Mechanobiology in Muscle and Nerve, PLoS One. 7 (2012). https://doi.org/10.1371/journal.pone.0051499.

[38] J.T. Feng, Y.P. Zhao, Influence of different amount of Au on the wetting behavior of PDMS membrane, Biomed. Microdevices. 10 (2008) 65–72. https://doi.org/10.1007/s10544-007-9110-2.

[39] T. Razafiarison, U. Silván, D. Meier, J.G. Snedeker, Surface-driven collagen self-assembly affects early osteogenic stem cell signaling, Adv. Healthc. Mater. 5 (2016) 1481–1492. https://doi.org/10.1002/adhm.201600128.

[40] P. Ferreira, Á. Carvalho, T.R. Correia, B.P. Antunes, I.J. Correia, P. Alves, Functionalization of polydimethylsiloxane membranes to be used in the production of voice prostheses, Sci. Technol. Adv. Mater. 14 (2013). https://doi.org/10.1088/1468-6996/14/5/055006.

[41] C.F. Araujo, J.A.P. Coutinho, M.M. Nolasco, S.F. Parker, P.J.A. Ribeiro-Claro, S. Rudić, B.I.G. Soares, P.D. Vaz, Inelastic neutron scattering study of reline: Shedding light on the hydrogen bonding network of deep eutectic solvents, Phys. Chem. Chem. Phys. 19 (2017) 17998–18009. https://doi.org/10.1039/c7cp01286a.

[42] C. Yuan, K. Chu, H. Li, L. Su, K. Yang, Y. Wang, X. Li, In situ Raman and synchrotron X-ray diffraction study on crystallization of choline chloride/urea deep eutectic solvent under high pressure, Chem. Phys. Lett. 661 (2016) 240–245. https://doi.org/10.1016/j.cplett.2016.04.011.

[43] S. Zhu, H. Li, W. Zhu, W. Jiang, C. Wang, P. Wu, Q. Zhang, H. Li, Vibrational analysis and formation mechanism of typical deep eutectic solvents: An experimental and theoretical study, J. Mol. Graphics Modell. 68 (2016) 158–175. https://doi.org/10.1016/j.jmgm.2016.05.003.

[44] Í.F.T. de Souza, M.C.C. Ribeiro, A Raman spectroscopy and rheology study of the phase transitions of the ionic liquid choline acetate, J. Mol. Liq. 322 (2021). https://doi.org/10.1016/j.molliq.2020.114530.

[45] C. Hisatsune, Low-temperature infrared study of ammonium carbamate formation, Can. J. Chem. 62 (1984) 945–948. https://doi.org/10.1139/v84-155.

[46] V. Souchon, M.D.O. de Aleixo, O. Delpoux, C. Sagnard, P. Mougin, A. Wender, L. Raynal, In situ determination of species distribution in alkanolamine-H_2O-CO_2 systems by Raman spectroscopy, in: Energy Procedia, Elsevier Ltd, (2011) 554–561. https://doi.org/10.1016/j.egypro.2011.01.088.

[47] F. Mani, M. Peruzzini, P. Stoppioni, CO_2 absorption by aqueous NH_3 solutions: Speciation of ammonium carbamate, bicarbonate and carbonate by a ^{13}C NMR study, Green Chem. 8 (2006) 995–1000. https://doi.org/10.1039/b602051h.

[48] J.H. Liao, P.C. Wu, Y.H. Bai, Eutectic mixture of choline chloride/urea as a green solvent in synthesis of a coordination polymer: [$Zn(O_3PCH_2CO_2)$]·NH_4, Inorg. Chem. Commun. 8 (2005) 390–392. https://doi.org/10.1016/j.inoche.2005.01.025.

[49] S.P. Simeonov, C.A.M. Afonso, Basicity and stability of urea deep eutectic mixtures, RSC Adv. 6 (2016) 5485–5490. https://doi.org/10.1039/c5ra24558c.

[50] D.R. Lide, ed., Vapor pressure of water from 0 to 370°C, in: CRC Handbook of Chemistry and Physics, 88th Ed. 2007-2008, CRC, Taylor & Francis, Boca Raton, FL. (2008) 6–11.

[51] B.E. Poling, G.H. Thomson, D.G. Friend, R.L. Rowley, W.V. Wilding, Physical and Chemical Data, in: D.W. Green, R.H. Perry (Eds.), Perry's Chemical Engineers' Handbook, 8th Ed., McGraw-Hill, New York, (2007) 2–93.